CMLS, Cell. Mol. Life Sci. 61 (2004) 982–991
1420-682X/04/080982-10
DOI 10.1007/s00018-003-3447-3

CMLS Cellular and Molecular Life Sciences

Research Article

Investigation of the effects of copper ions on protein aggregation using a model system

C. Capanni [a], N. Taddei [a,*], S. Gabrielli [b], L. Messori [b], P. Orioli [b], F. Chiti [a], M. Stefani [a] and G. Ramponi [a]

[a] Dipartimento di Scienze Biochimiche, Università di Firenze, Viale Morgagni 50, 50134 Firenze (Italy),
Fax: +39 055 4222725, e-mail: taddei_n@scibio.unifi.it
[b] Dipartimento di Chimica, Polo Scientifico, Università di Firenze, Sesto F.no, Firenze (Italy)

Received 4 December 2003; received after revision 7 January 2004; accepted 3 February 2004

Abstract. Protein aggregation is a notable feature of various human disorders, including Parkinson's disease, Alzheimer's disease and many others systemic amyloidoses. An increasing number of observations in vitro suggest that transition metals are able to accelerate the aggregation process of several proteins found in pathological deposits, e.g. α-synuclein, amyloid β (Aβ) peptide, β_2-microglobulin and fragments of the prion protein. Here we report the effects of metal ions on the aggregation rate of human muscle acylphosphatase, a suitable model system for aggregation studies in vitro. Among the different species tested, Cu^{2+} produced the most remarkable acceleration of aggregation, the rate of the process being 2.5-fold higher in the presence of 0.1 mM metal concentration. Data reported in the literature suggest the possible role played by histidine residues or negatively charged clusters present in the amino acid sequence in Cu^{2+}-mediated aggregation of pathological proteins. Acylphosphatase does not contain histidine residues and is a basic protein. A number of histidine-containing mutational variants of acylphosphatase were produced to evaluate the importance of histidine in the aggregation process. The Cu^{2+}-induced acceleration of aggregation was not significantly altered in the protein variants. The different aggregation rates shown by each variant were entirely explained by the changes of hydrophobicity or propensity to form a β structure introduced by the point mutation. The effect of Cu^{2+} on acylphosphatase aggregation cannot therefore be attributed to the specific factors usually invoked in the aggregation of pathological proteins. The effect, rather, seems to be a general related to the chemistry of the polypeptide backbone and could represent an additional deleterious factor resulting from the alteration of the homeostasis of metal ions in cells.

Key words. Protein aggregation; protein misfolding; amyloid fibrils; Cu^{2+}; metal ions.

Various human disorders, such as Parkinson's disease (PD) and Alzheimer's disease (AD), are associated with the formation of stable protein aggregates, known as amyloid fibrils, resulting from misfolding processes [1–5]. Although each disorder is associated with a particular protein, the fibrils show, in the different pathologies, common structural features [6, 7]. Amyloid aggregation has been described for various proteins, including those that are not involved in any disease. It is now considered a common property of polypeptide chains, acting in competition with the normal folding pathway [8]. Recent reports concerning proteins associated with diseases as well as non-pathological proteins suggest that the species actually toxic for living systems are prefibrillar, relatively ordered, aggregates rather than mature, fully ordered, amyloid fibrils [9–12]. Such results underline the importance of studying the early stages of protein aggregation to gain an understanding of the pathogenic mechanisms of amyloid diseases [13].

* Corresponding author.

An increasing number of observations indicate that transition metals, in their di- and trivalent ionic form, are capable of accelerating the aggregation process of various pathologic proteins, e.g. α-synuclein (α-syn), the amyloid β peptide (Aβ), β_2-microglobulin (β2-m) and fragments of the prion protein (PrP) [14–18].

α-syn is a small protein abundant in various regions of the brain [19, 20]. It belongs to the family of natively unfolded proteins [21, 22] and is involved in the formation of abnormal protein depositions, by precipitating in senile plaques and Lewy bodies in AD and PD, respectively [23–25]. In vitro aggregation of α-syn is modulated by various factors, including transition metals [14, 15, 26]. Another polypeptide whose aggregation has been found to be dependent on the presence of metal ions is Aβ, the major component of neocortical amyloid deposition in AD [27, 28]. Aβ precipitates in the presence of metals in vitro [16, 29–31]. β2-m is a protein that forms amyloid fibrils as a consequence of long-term hemodialysis [4, 32]. Binding of Cu^{2+} to β2-m results in the destabilization of the protein which facilitates amyloid formation [17].

Prion diseases are fatal neurodegenerative diseases in which the cellular isoform of the prion protein (PrP^{C}) undergoes a conformational transition, producing the pathogenic isoform (PrP^{Sc}), responsible for fatal neurodegenerative diseases, including Creutzfeld-Jakob disease in humans and spongiform encephalopathy in animals [33–35]. A synthetic peptide encompassing human PrP residues 106–126 (PrP106–126) is highly fibrillogenic and toxic to neurons in vitro [36, 37]. It therefore represents a suitable model peptide for studying PrP^{Sc} aggregation [36, 38, 39]. A recent study investigating the effect of metals on PrP106–126 aggregation showed that copper, and to a lesser extent zinc, can promote peptide fibrilization [18].

To assess whether metal-induced aggregation is a general phenomenon for polypeptide chains or is specific to the few systems mentioned above, we studied the effect of metal ions on the aggregation rate of human muscle acylphosphatase (AcP), a relatively simple protein that represents a suitable model system for aggregation studies in vitro [40–42]. AcP is an α/β 99-residue protein lacking complicating factors such as disulfide bridges or bound cofactors [43] (fig. 1). Under appropriate conditions in vitro, AcP was shown to aggregate promptly into granular ordered species that in a few weeks rearrange and form amyloid fibrils structurally similar to those associated with disease [40]. Partial denaturation of the native state is required for aggregation, as indicated by the need to employ non-aggressive denaturants or destabilizing mutations to induce aggregation from this protein [40, 41]. Once the native state is denatured, aggregation is an ordered process promoted by specific regions of the protein sequence that are distinct from those containing residues that determine the rate of its folding [42]. Such regions, encompassing residues 16–31 and 87–98, are characterized by a relatively high hydrophobicity and propensity to form a β sheet structure, and are thought to be relatively exposed to the solvent [42].

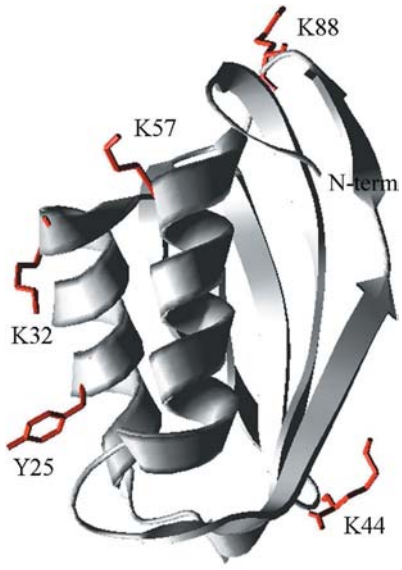

Figure 1. Schematic representation of AcP structure. The side chains of replaced residues are highlighted.

Here we investigated the effects of several metal ions on the early stages of AcP aggregation focusing our attention on Cu^{2+} and on the possible role played by histidine residues in the Cu^{2+}-mediated aggregation of the protein. Unlike Aβ, α-syn, β2-m and a prion fragment, the proteins previously shown to aggregate more readily following the addition of heavy metal ions, AcP presents no histidines and displays an overall positive net charge. It therefore represents a useful model system to assess the mechanisms by which metals induce aggregation, in particular, whether binding of metals to histidine residues or clusters of negatively charged residues represents a general mechanism by which metals favor aggregation.

Materials and methods

Mutant production and purification

All mutants were produced using the QuickChange site-directed mutagenesis kit from Stratagene. DNA sequencing confirmed the presence of the desired mutations. All AcP proteins used in this study contain a serine at position 21, instead of a cysteine residue. This substitution eliminates the complexities associated with the presence of a cysteine residue [44]. We refer to the protein with only the C21S mutation as the wild-type AcP throughout the text. Cloning, expression and purification of the wild-type and mutated AcP were done as described by Taddei

et al. [45]. SDS-polyacrylamide gel electrophoresis was used to check protein purity. The protein concentration was determined by UV absorption using an ε_{280} value of 1.49 ml mg^{-1} cm^{-1}.

Equilibrium experiments

Equilibrium denaturation curves of wild-type AcP and its variants were obtained by determining the fluorescence of 25–28 equilibrated samples containing 0.02 mg ml^{-1} AcP in 50 mM acetate buffer (pH 5.5, 28 °C) and various urea concentrations ranging from 0 to 8.1 M. A Shimatzu RF 5000 spectrofluorophotometer was used, with excitation and emission wavelengths of 280 and 335 nm, respectively. Urea denaturation curves, representing the change of fluorescence as a function of urea concentration, were fitted and analyzed according to the method of Santoro and Bolen [46]. With this procedure one can obtain the following thermodynamic parameters: the free energy of unfolding in the absence of denaturants (ΔG^{H2O}), the dependence of ΔG on denaturant concentration (*m* value) and the urea concentration at which half of the protein molecules are denatured (C_m). C_m was determined by dividing ΔG^{H2O} by the *m* value obtained from the fitting. In this work an averaged value for *m* was calculated to redetermine ΔG^{H2O} more accurately.

Aggregation kinetics

Aggregation of AcP and its variants was initiated by incubating the protein at a concentration of 0.4 mg ml^{-1} in 25% (v/v) 2,2,2-trifluoroethanol (TFE), 50 mM acetate buffer pH 5.5, 25 °C. When aggregation was studied in the presence of metal ions, this incubating solution also contained the desired concentration (0.1, 1 or 5 mM) of the various metal ions in the form of chloride salts. Aliquots of 60 µl of this solution were mixed, at regular time intervals, with 440 µl of 25 mM phosphate buffer, pH 6.0, containing 25 µM thioflavin T (ThT). The resulting fluorescence was measured using a Shimatzu RF 5000 spectrofluorimeter thermostated at 25 °C. Excitation and emission wavelengths were 440 and 485, respectively. Plots of fluorescence versus time were fitted to single exponential functions to determine *k* values, i.e. the rate constants of aggregation.

Far-UV circular dichroism

Far-UV circular dichroism (CD) spectra were acquired after fixed time intervals during aggregation. The CD experiments were carried out on a Jasco J-810 spectropolarimeter, thermostated with a water-circulating bath, using 1-mm path length quartz cuvettes. AcP was incubated at a concentration of 0.4 mg ml^{-1} in 25% (v/v) TFE, 50 mM acetate buffer pH 5.5, 25 °C, in the absence or presence of 0.1 mM copper ions. Aliquots were withdrawn at regular time intervals for far-UV CD analysis in the range 200–250 nm. The changes in the CD spectrum of AcP incubated under these conditions were followed for about 3 h. Mean residue ellipticity [θ] data were calculated as follows:

$$[\theta] = \theta / (10 \times c \times l \times n)$$

where θ represents the ellipticity raw data, c is the molar concentration of the samples, l is the path length and n is the number of residues of the protein.

Transmission electron microscopy

Electron micrographs were acquired using a Joel JEM 1010 transmission electron microscope at 80 kV excitation voltage. Samples at a 0.4 mg ml^{-1} concentration of protein were incubated for various time periods at 25 °C in 50 mM acetate buffer, pH 5.5, in 25% (v/v) TFE, in the absence or presence of 0.1 mM Cu^{2+}. Three-microliter volumes of the protein samples were placed for 3/5 min on a formvar/carbon-coated grid. Samples were then negatively stained with 3 µl 2% uranyl acetate and observed at magnifications ranging from 15,000 to 40,000.

Results

AcP aggregation is influenced by the presence of metal ions

AcP aggregates in aqueous solutions containing 25% (v/v) TFE at pH 5.5 [40]. At the protein concentration used in this study, TFE denatures AcP within a few seconds and aggregation occurs subsequently on a much longer time scale. We centered our attention on the first aggregational events leading to non-fibrillar (granular) aggregates. Such species have previously been demonstrated to evolve into amyloid fibrils [40]; more important, AcP forms granular aggregates morphologically similar to those produced from HypF-N, a protein belonging to the acylphosphatase superfamily. Such aggregates have been indicated as the actual toxic species for cells [12]. These experimental conditions allow the aggregation process to be followed under conditions in which the native state of AcP is not significantly populated. Any change of aggregation rate observed as a result of mutation or addition of metal ions can therefore be entirely attributed to the effect of these modifying agents on the self-assembly of the denatured polypeptide chains, rather than on the stability of the native state. The aggregation process of AcP can be followed using a simple optical test based on the ability of a specific dye, ThT, to bind amyloid aggregates specifically [42]. The rate of aggregation of wild-type AcP was measured in the presence of several metal cations added to the incubation mixture as chloride salts. We initially added each salt at a 5 mM concentration to the aggregation solution. Although this metal concentration is considerably higher than that found in the physiological fluids of the human body [47],

it was chosen for a preliminary indication of the effects of various cations. All metal ions used here led to an increase in the aggregation rate of AcP (table 1). The aggregation rate in the presence of Cu^{2+}, Fe^{2+} and Cd^{2+} occurred on a timescale that was too rapid to allow the actual measurement of the rate constant. The presence of Zn^{2+} in the reaction mixture caused a decrease in ThT fluorescence, presumably due to complex effects which we have not investigated further.

Aggregation of AcP in the presence of Cu^{2+}

In the light of this preliminary screening, we decided to analyze the influence of copper ions on the aggregation rate of AcP. Copper is an essential element for life. It is widely distributed in plants and animals and plays a critical role in human metabolism. Cu^{2+} metal ions exist in a chelated form, in vivo, bound to ceruloplasmin and other biomolecules such as albumin, transcuprein, peptides and amino acids [47]. As already mentioned, Cu^{2+} has been implicated in the pathogenesis of several diseases characterized by deposition of amyloid material [15, 17, 29, 48]. Varying concentrations of copper ions have been found physiologically throughout the body: 16–20 µM in blood, 15 µM in the synaptic cleft and 0.5–2.5 µM in cerebrospinal fluid [47]. Since 5 mM Cu^{2+} induces a too marked acceleration of AcP aggregation and is also several orders of magnitude higher than the physiological concentrations, we progressively lowered the concentration of Cu^{2+} to 1 and 0.1 mM, to approach the physiological concentrations of the metal. At 1 mM, the kinetics of the aggregation process were still too rapid to be measured accurately. At 0.1 mM Cu^{2+}, the observed acceleration is about 2.5-fold compared to the control experiment in the absence of Cu^{2+} (table 2, fig. 2). Far-UV CD spectra were acquired at fixed time intervals after the initiation of the aggregation process in the absence or presence of Cu^{2+} (fig. 3). Both spectra at 1 min are indicative of a high content of α-helical structure as expected for AcP molecules denatured in the presence of TFE [40]. After

Table 1. Aggregation rate constants (k) of wild-type AcP in the presence of various metal ions at a 5 mM concentration.

Metal ions	k (s^{-1})
Control	0.00073
Co^{2+}	0.00174
Ca^{2+}	0.00122
Cu^{2+}	≫
Fe^{3+}	≫
Cd^{2+}	≫
Mg^{2+}	0.00157
Mn^{2+}	0.00283
Ni^{2+}	0.00146
Zn^{2+}	n.d.

Experimental errors for rate measurements are ± 7%; ≫, unmeasurable rates (too fast); n.d., not determined.

Table 2. Aggregation rate constants of all AcP variants in the absence (k) and presence (k_{Cu}) of 0.1 mM Cu^{2+}, at pH 5.5 and 7.4.

	Protein variant	k (s^{-1})	k_{Cu} (s^{-1})	k_{Cu}/k
pH 5.5	WT	0.00073	0.00186	2.6
	Y25H	0.00004	0.00046	11.3
	K88H	0.00194	0.00682	3.5
	Y25H/K88H	0.00121	0.00365	3.0
	K32H	0.00411	0.00544	1.3
	K44H	0.00139	0.00190	1.4
	K57H	0.00122	0.00308	2.5
pH 7.4	WT	0.00038	0.00144	3.8
	Y25H	0.00020	0.00096	4.8
	K88H	0.00498	0.00927	1.9
	Y25H/K88H	0.00111	0.00211	1.9

Experimental errors for rate measurements are ± 7%.

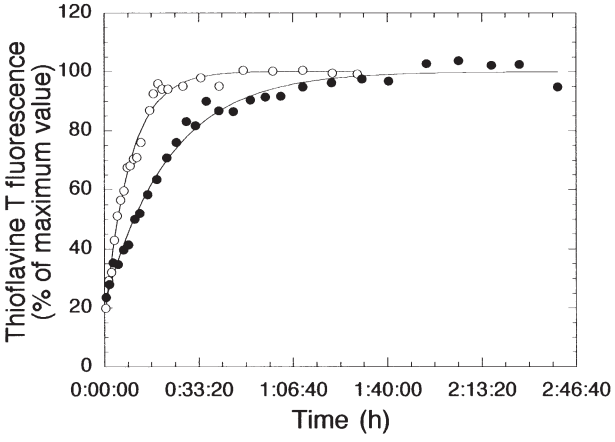

Figure 2. Rate of aggregation of wild-type AcP in the absence (filled circles) and presence (open circles) of 0.1 mM Cu^{2+}. The continuous lines are the best fits of the data points to single exponential functions. The aggregation rates were measured by following the increase of ThT fluorescence at 485 nm.

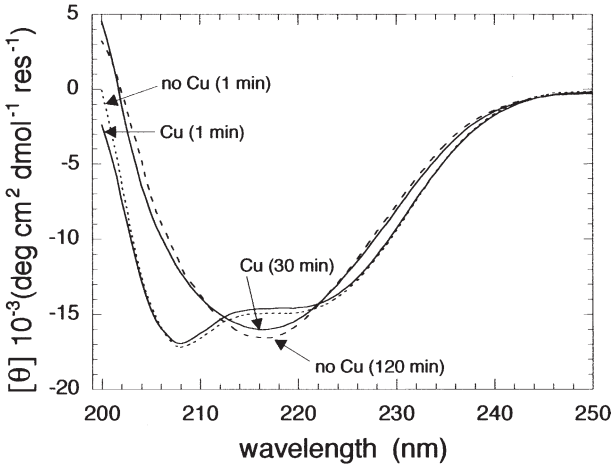

Figure 3. Far-UV CD spectra of AcP during aggregation in the presence and absence of Cu^{2+} at different time intervals. See Materials and methods for experimental details.

30 min, the CD spectrum of the protein incubated in the presence of Cu^{2+} suggests that a structural rearrangement has produced species rich in β structure. The same spectrum is observable only after 120 min for protein molecules incubated in the absence of Cu^{2+} (fig. 3). These results indicate a more rapid transition in the presence of copper ions as shown by ThT-binding experiments. The electron micrographs in figure 4 show the presence of granular aggregates of similar morphology after 30-min and 2-h incubation in the presence and absence of Cu^{2+}, respectively.

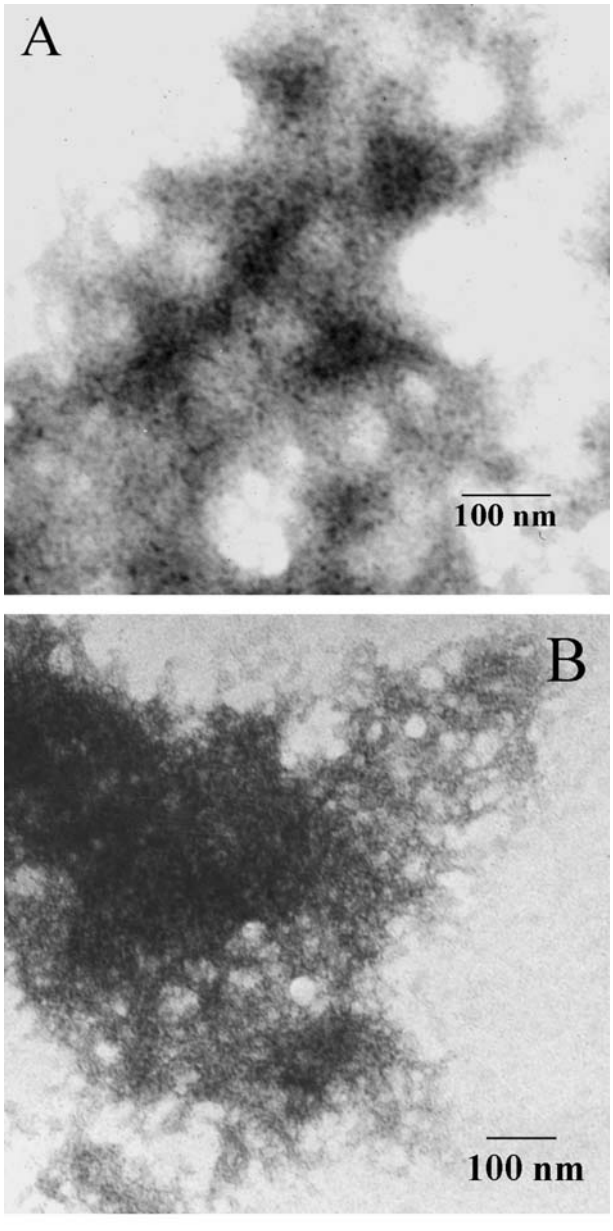

Figure 4. Transmission electron micrograph of AcP aggregates after incubation in 50 mM acetate pH 5.5 containing 25 % TFE: 2 h no Cu^{2+} (*A*); 30 min 0.1 mM Cu^{2+} (*B*). The length of the solid bars is 100 nm.

Aggregation of histidine-containing AcP variants in the presence of Cu^{2+}

Wild-type AcP lacks histidine residues. Histidine residues have been suggested to be involved in the copper-mediated aggregation of proteins through their ability to coordinate copper ions [17, 18, 48, 49]. To investigate whether His residues could have a relevant role in increasing the aggregation rate of AcP through a specific mechanism of copper binding, we substituted some selected residues with histidines in different regions of the protein. A list of the mutants together with their observed aggregation rates in the presence and absence of 0.1 mM Cu^{2+} is reported in table 2. With the exception of the substitution Y25H, all the mutations were designed to introduce a Lys to His substitution to keep the total charge of AcP unaltered, at least at the pH value of 5.5 used here. The Y25H, K32H and K88H substitutions involve residues belonging to regions of the sequence that have been shown to be crucial for AcP aggregation; on the other hand, the K44H and K57H replacements are located in regions that are thought to be less relevant for this process [42]. A protein variant carrying a double mutation, Y25H/K88H, was also designed to probe the possible formation of a bridge, mediated by Cu^{2+}.

The conformational stability of AcP variants was determined by means of equilibrium urea denaturation experiments at pH 5.5 and 28 °C, as described in Materials and methods. Under these experimental conditions, urea denaturation is a completely reversible process. The urea denaturation curves of wild-type AcP and its variants are reported in figure 5 and the relevant thermodynamic parameters, evaluated with the fitting procedure described by Santoro and Bolen [46], are listed in table 3. The dependence of the free energy of unfolding on urea concentration, i.e. the *m* value, is very similar, within the experimental error, for all the species studied and an averaged *m* value was used to estimate the conformational stability of protein variants. The K44H variant is slightly stabilized compared to the wild-type protein, while K57H and Y25H were destabilized. The conformational stability of K32H, K88H and Y25H/K88H variants is not significantly different from that of the wild-type protein. All protein variants showed a catalytic activity comparable to that of the wild-type protein. These data, together with conformational stability, demonstrate that the overall structure of all mutational variants studied here is substantially similar to that of the wild type.

All protein variants have an aggregation rate in the absence of copper significantly different from that of the wild-type protein (table 2). Explanations for this behavior will be discussed below. The kinetic measurements were repeated in the presence of 0.1 mM Cu^{2+}. The results, summarized in table 2, show that the addition of the cation to the protein variants results in an enhancement of aggregation rates similar, proportionately, to the wild-

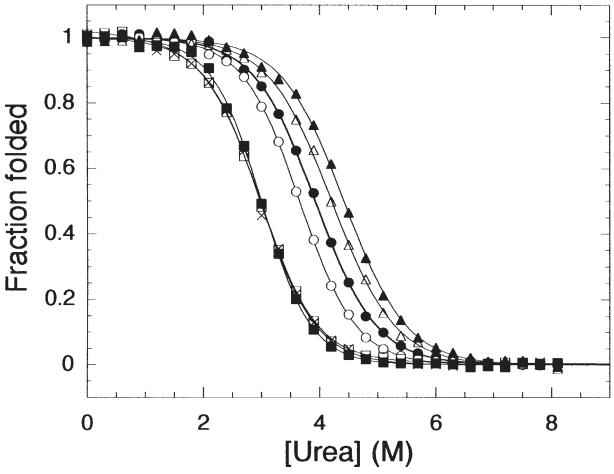

Figure 5. Equilibrium urea-induced denaturation of AcP and its variants at 28 °C in 50 mM acetate buffer (pH 5.5), monitored by intrinsic tryptophan fluorescence changes at 335 nm. The proteins are: wild type AcP (filled circles), Y25H (crosses), K32H (open circles), K44H (filled triangles), K57H (filled squares), K88H (open triangles), Y25H/K88H (open squares). The raw data have been converted to the fraction of folded protein using: $f_f = (y_d - y)/(y_d - y_n)$, where y_n and y_d are the signals of the native and denatured protein, respectively, extrapolated to the urea concentration under consideration.

Table 3. Thermodynamic parameters of AcP variants obtained by equilibrium unfolding experiments.

Protein variant	C_m (M)	m (kJ mol^{-1} M^{-1})	ΔG^{H2O} (kJ mol^{-1})
WT	3.93	4.76	19.8
Y25H	2.97	5.23	15.0
K32H	3.66	5.13	18.4
K44H	4.40	4.64	22.1
K57H	3.00	5.81	15.1
K88H	4.21	4.62	21.2
Y25H/K88H	3.26	5.05	16.4

C_m is the urea concentration required to unfold 50% of the protein molecules. Experimental error is ± 0.15 M. m is the dependence of ΔG on urea concentration. Experimental error is ± 5%. ΔG^{H2O} is the free energy of unfolding in the absence of urea. The m value is similar, within the experimental error, for all the species studied and an averaged m value (5.03) was used to estimate the conformational stability. Experimental errors for ΔG^{H2O} values are ± 10%.

type protein. An exception is, again, represented by the Y25H variant whose aggregation rate was accelerated by the presence of Cu^{2+} more markedly than other species (ca 11-fold). The Y25H/K88H variant showed an aggregation rate which is an average between the rates of the Y25H and K88H single variants. Overall, the presence of histidine residues at different locations in the AcP sequence does not seem to influence significantly the aggregation process mediated by the presence of Cu^{2+}. Even the double mutant Y25H/K88H, which contains two histidine residues, does not have a copper-induced acceleration of aggregation significantly higher than that observed for the wild-type protein. Moreover, the experiments performed at pH 7.4 produced similar results indicating that the ionization degree of the His residue is not, at least in our case, a factor that can influence aggregation in the presence of Cu^{2+}.

Effect of the mutations on AcP aggregation

In the absence of Cu^{2+}, all protein variants show an increase in the aggregation rate, with the exception of the Y25H variant, which aggregates about 18-fold slower than wild-type AcP (table 3). Among the variants with an accelerated aggregation, the K32H and K88H mutants show the most remarkable effects. The smaller changes in aggregation rate resulting from the K44H and K57H replacement can be, in part, attributed to the observation that these substitutions involve residues thought to be less relevant in the aggregation process of AcP [42]. The aggregation rate of the Y25H/K88H variant is intermediate between those of the corresponding single mutants. The observed changes of aggregation rate following these mutations can be explained by taking into account the effect of the amino acid substitutions on three simple physical parameters, hydrophobicity, secondary-structure propensities and charge [42, 50]. Table 4 summarizes the effects of any given substitution on α-helical and β sheet propensity and hydrophobicity. All protein variants were found to be catalytically active, indicating that the global native-like architecture is conserved in all cases. The use of the simple equation introduced by Chiti and coworkers [50] allows the aggregation rate to be estimated on the basis of the change of these three factors. The theoretical results, reported in table 4, are in good agreement with the experimental ones, suggesting that the changes in aggregation rates can be explained in terms of changes in these basic physical factors. The Y25H variant, for example, displays a dramatically reduced aggregation rate because the Tyr to His substitution introduces a marked decrease in hydrophobicity, a small increase in α-helical propensity, a decrease in β sheet propensity and an increase in the total charge of the protein. All these changes, taken as a whole, counter the aggregation process and the protein variant carrying the substitution is, therefore, slower to aggregate. A slower aggregation for this mutant is both observed experimentally and predicted theoretically using the equation (table 4).

The theoretical aggregation rate estimated for the K32H variant is, however, lower than that calculated experimentally (table 4). Clues to explain this discrepancy come from suggestions that His32 could be deprotonated under the experimental conditions, although the pH value of 5.5 employed here would suggest that it is indeed protonated. If the equation is used after considering that the newly inserted histidine residue is deprotonated, the theoretical value is much closer to that obtained experimentally. To

validate this view, aggregation rates were measured at pH 7.4 for some mutants, a pH at which His residues are supposed to be deprotonated [51]. For the K88H variant, the increse in the aggregation rate relative to the wild-type protein is more marked at pH 7.4 than at pH 5.5 (table 4). Similarly, for the Y25H variant, the decrease in aggregation rate relative to the wild-type protein is less marked at pH 7.4 than at pH 5.5 (table 4). The acceleration of aggregation for these two mutants at pH 7.4 can be ascribed to a positive contribution to aggregation conferred by deprotonated histidine residues, relative to the protonated side chain expected at pH 5.5. The theoretical predicted values confirm the observation trends, confirming the important role of residue ionization state in the aggregation process. Interestingly, the aggregation rate of the K32H mutant does not change significantly upon shift of the pH, confirming our hypothesis that His32 is deprotonated at both pH values.

Discussion

Under the experimental conditions used in this work, AcP aggregation begins with the formation of granular and protofibrillar aggregates in which a substantial amount of β structure is present [40]. In the absence of metal ions, this process occurs within a few hours, evolving further, on the timescale of weeks, to the formation of more organized fibrillar structures. A similar behavior has been observed for proteins of clinical relevance, such as the Aβ peptide and α-syn [9, 52]. In both these systems, protofibrillar aggregates develop prior to the formation of mature amyloid fibrils; interestingly, the formation of such oligomeric prefibrillar aggregates has been indicated as a possible therapeutical target for the control of disease progression [52]. A 'new view' for amyloid diseases is depicted in a recent review that underlines the importance of the prefibrillar aggregates as toxic species and a common origin of such pathological conditions [13]. All these considerations enable us to consider AcP as a simplified model system to gain insights into the early events of aggregation associated with protein-misfolding diseases.

Mechanisms of Cu^{2+}-induced aggregation in proteins

The effects of metal ions on protein aggregation have been investigated for different protein systems, particularly for proteins that are known to be directly involved in protein deposition diseases. Several possible mechanisms have been described to account for metal-stimulated aggregation of α-syn [14, 15, 26]. A systematic analysis of the effects of various metal ions has shown that they can directly accelerate α-syn aggregation by inducing formation of a partially folded intermediate which represents the critical precursor to fibrils [26]. On the other hand, metal ions have been proposed to interact with the C-terminal acidic region of the protein, which provides a negatively charged surface, causing α-syn to be oxidized and consequently self-assemble [15]. Metals such as iron and copper ions react with hydrogen peroxide to produce hydroxyl radicals which can induce the oxidative modification of DNA, protein and lipids [53, 54]. These radicals can also lead to cross-linking and aggregation of amyloidogenic molecules [55]. There is also a growing body of data indicating that, during exposure to hydrogen peroxide, many proteins with metal-binding sites can undergo oxidative damage and release metal ions [56]. For example, the oxidative modification of Cu,Zn-superoxide dismutase and of ceruloplasmin induces the release of copper ions [57, 58], which can influence the aggregation process.

At pH 5.5, AcP is a positively charged protein, displaying an overall net charge of +5. Analysis of the sequence of AcP does not reveal clusters of negative charges that, in a denatured or partially denatured state, could provide a negative surface for copper binding as was proposed for α-syn. Moreover, the overall net charge has previously been shown to be an important factor that influences the aggregation rate of a protein [59]. A high net charge sets up electrostatic repulsions within the population of un-

Table 4. Effects of amino acid substitution on hydrophobicity, secondary-structure propensities and charge, and comparison between theoretical and experimental changes in aggregation rates.

Mutation	$\Delta Hydr$ (kJ mol^{-1})*	$\Delta\Delta G_{\beta\,\mathrm{coil}}$ (kJ mol^{-1})*	$\Delta\Delta G_{\mathrm{coil}\,\alpha}$ (kJ mol^{-1})*	$\Delta Charge$	Theoretical (k_{mut}/k_{wt})	Experimental (k_{mut}/k_{wt})
Y25H	–4.34	–3.06	0.83	–1	–2.79	–2.89
K32H	–0.10	–0.41	2.74	0	0.40	1.73
K44H	–0.10	–0.41	2.96	0	0.44	0.64
K57H	–0.10	–0.41	3.73	0	0.59	0.51
K88H	–0.10	–0.41	2.43	0	0.34	0.98
K32H(deprot)	2.13	–0.41	2.74	1	1.32	1.74
Y25H(deprot)	–2.11	–3.55	1.01	0	–1.84	–1.29
K88H(deprot)	2.13	–0.41	2.10	1	1.19	1.92

* Data taken from Chiti et al. [50].

folded or partially unfolded molecules from which aggregation takes place. This inhibits the intermolecular interactions that underlie the aggregation process. In agreement with this proposal, an increase in the net charge of AcP by mutation significantly slows the aggregation process [59]. The difficulty for a positively charged protein to bind copper by a mechanism of electrostatic interaction and the inhibition that would result on the aggregation process from such binding due to an overall increase in charge clearly suggest that the Cu^{2+}-mediated acceleration of AcP aggregation cannot be explained by a simple electrostatic argument. This does not exclude the possibility that proteins displaying a positive net charge and dispersed negative residues aggregate from a partially structured or native-like state in which negatively charged binding pockets arise from clusters of acidic residues.

The binding of Aβ to metal ions results in Aβ assembly [48, 49]. Such binding has been shown to involve multiple copper ions, through the coordination to some histidine residues [60]. In addition to favoring progression of AD by increasing the propensity of Aβ to self-assemble, evidence is mounting that Cu^{2+} also induces oxidative stress in the neurodegeneration of AD [61, 62]. Extensive redox chemical reactions take place when Aβ binds Cu^{2+} and Fe^{3+} [63]. Such binding reduces the oxidation state of both metals, therefore triggering reduction of O_2 to H_2O_2 [63]. The oxidative stress observed in AD [61, 62] can therefore be related to the production of reactive oxygen species by metal-bound forms of Aβ. In β2-m, the histidine residues at positions 13 and 31 seem to be involved in the binding of Cu^{2+} [17]. A similar concept holds for PrP: the key residue for metal binding and aggregation is represented by a histidine residue, namely His111 [18]. Nevertheless, in this case, the N-terminal amino group and the methionine residue at position 112 also seem to have a relevant role [18].

Unlike α-syn, Aβ, β2-m and PrP, AcP contains no histidine residues. The ability of Cu^{2+} to accelerate aggregation of AcP indicates that this ion favors the aggregation process of polypeptide chains by mechanisms that are, at least in part, unrelated to histidine binding. Of interest in this regard is that all the histidine-containing variants of AcP produced in this study are accelerated by Cu^{2+} to a similar extent as the wild-type protein (table 2). Copper binding to histidine residues, whenever present, would represent a specific mechanism for a restricted number of proteins, resulting in a more rapid and effective aggregation of the polypeptide chains.

These observations suggest that the effect of Cu^{2+} on AcP aggregation cannot be attributed to the specific factors usually invoked for the aggregation of several pathological proteins. Rather, it seems to be a more general effect related to the chemistry of the polypeptide backbone or to a variety of non-specific effects, e.g. binding to side chains of amino acid residues commonly distributed in polypeptide chains [64].

Cu^{2+} levels and protein aggregation

The Cu^{2+} concentration used in our experiments (0.1 mM) is significantly higher than that normally present in the human body, which is about 15–20 µM [47]. When AcP is incubated in an aggregation solution containing 0.1 mM Cu^{2+}, the rate of aggregation appears to be accelerated by about 2.5 fold, compared to the control experiment in the absence of the cation. Unlike other proteins, such as Aβ peptide, α-syn, β2-m and PrP, for which concentrations of Cu^{2+} similar to physiological ones are sufficient to promote aggregation [17, 48, 65], the rate of this process for AcP increases only with higher concentrations of copper. The lower sensitivity of the aggregation process of AcP to copper, relative to other protein systems, is likely due to the absence of a specific binding mechanism for this metal ion in the AcP sequence.

The fact remains, however, that the absence of specific binding sites or regions does not completely suppress the aggregation-promoting effects of Cu^{2+}. Cu^{2+} is therefore a rather dangerous metal in vivo, capable of promoting a rather general protein aggregation. These dangerous effects could explain why proteins able to chelate metals in vivo, such as ceruloplasmin, albumin and transcuprein, as well as other peptides and amino acids, are necessary in living organisms [47]. The presence of these proteins maintains a low concentration of free copper in the body. Our results, together with those obtained for other proteins, suggest that an abnormal copper homeostasis could represent a risk factor for aggregation processes.

The question naturally arises as to whether these in vitro observations have clinical relevance. Studies in mice and humans show that iron and copper levels increase with normal aging in several tissues, including the brain [66, 67]. Recent analyses have shown that the concentration of several heavy metals is significantly increased in the brain of AD and PD patients [68–70]. Moreover, a positive correlation between the incidence of PD and industrialization has been recognized [71]. For example, analysis of the PD mortality in Michigan (1986–1988) with respect to potential heavy metal exposure, revealed that counties with an industry in paper, chemical, iron or copper-related industrial categories had significantly higher PD death rates than counties without these industries [72]. Other studies have established that an increased risk for PD is associated with occupational exposure to metals such as manganese, iron, aluminum and copper [73, 74]. Exposure to metal ions has, therefore, been proposed as a risk factor for neurodegenerative diseases [26].

Acknowledgements. The authors wish to thank Dr C. Parrini for technical assistance during the experimental work. Electron mi-

croscopy was carried out at the Dipartimento di Anatomia, Istologia e Medicina legale of the Università di Firenze. This work was supported by grants from MIUR (PRIN 2002 project 'Folding e misfolding di proteine: biogenesi, struttura e citotossicità di aggregati proteici'; FIRB project 'Protein folding: the second half of the genetic code'), from MIUR-CNR (L. 449/97, settore 'Genomica funzionale', progetto 'Strutture ed interazioni di prodotti genici'). N. T.'s research is supported in part by the Ente Cassa di Risparmio di Firenze (project 'Studio dei meccanismi molecolari alla base dell'aggregazione proteica e della formazione di fibrille amiloidi') and by the Compagnia di San Paolo (contract n. 2003.0727).

1 Kelly J. W. (1996) Alternative conformations of amyloidogenic proteins govern their behavior. Curr. Opin. Struct. Biol. **6:** 11–17.
2 Dobson C. M. (2001) The structural basis of protein folding and its links with human disease. Phil. Trans. R. Soc. Lond. B **356:** 133–145
3 Mattson M. P., Pedersen W. A., Duan W., Culmsee C. and Camandola S. (1999) Cellular and molecular mechanisms underlying perturbed energy metabolism and neuronal degeneration in Alzheimer's and Parkinson's diseases. Ann. NY Acad. Sci. **893:** 154–175
4 Bellotti V., Mangione P. and Stoppini, M. (1999) Biological activity and pathological implications of misfolded proteins. Cell. Mol. Life Sci. **53:** 977–991
5 Rochet J. C. and Lansbury P. T. Jr (2000) Amyloid fibrillogenesis: themes and variations. Curr. Opin. Struct. Biol. **10:** 60–68
6 Sunde M. and Blake C. C. P. (1997) The structure of amyloid fibrils by electron microscopy and X-ray diffraction. Adv. Protein Chem. **50:** 123–159
7 Serpell L. C., Sunde M., Benson M. D., Tennent G. A., Pepys M. B. and Fraser P. E. (2000) The protofilament substructure of amyloid fibrils. J. Mol. Biol. **300:** 1033–1039
8 Dobson C. M. (1999) Protein misfolding, evolution and disease. Trends Biochem. Sci. **9:** 329–332
9 Conway K. A., Lee S. J., Rochet J. C., Ding T. T., Williamson R. E. and Lansbury P. T. (2000) Acceleration of oligomerization, not fibrillization, is a shared property of both alpha-synuclein mutations linked to early-onset Parkinson's disease: implications for pathogenesis and therapy. Proc. Natl. Acad. Sci. USA **97:** 571–576
10 Bhatia R., Lin H. and Lal R. (2000) Fresh and nonfibrillar amyloid β protein (1–42) induces rapid cellular degeneration in aged human fibroblasts: evidence for AβP-channel-mediated cellular toxicity. FASEB J. **14:** 1233–1243
11 Sousa M. M., Cardoso I., Fernandes R., Guimaraes A. and Saraiva M. J. (2001) Deposition of transthyretin in early stages of familial amyloidotic polyneuropathy. Am. J. Pathol. **159:** 1993–2000
12 Bucciantini M., Giannoni E., Chiti F, Baroni F., Formigli L., Zurdo J. et al. (2002) Inherent toxicity of aggregates implies a common mechanism for protein misfolding diseases. Nature **416:** 507–511
13 Stefani M. and Dobson C. M. (2003) Protein aggregation and aggregate toxicity: new insights into protein folding, misfolding diseases and biological evolution. J. Mol. Med. **81:** 678–699
14 Hashimoto M., Hsu L. J., Xia Y., Takeda A. M., Sundsmo M. and Masliah E. (1999) Oxidative stress induces amyloid-like aggregate formation of NACP/alpha-synuclein in vitro. Neuroreport **10:** 717–721
15 Paik S. R., Shin H. J., Lee J. H., Chang C. S. and Kim J. (1999) Copper(II)-induced self-oligomerization of alpha-synuclein. Biochem. J. **340:** 821–828
16 Bush A. I., Moir R. D., Rosenkranz K. M. and Tanzi R. E. (1995) Zinc and Alzheimer's disease. Science **268:** 1921–1922
17 Morgan C. J., Gelfand M., Atreya C. and Miranker A. D. (2001) Kidney dialysis-associated amyloidosis: a molecular role for copper in fiber formation. J. Mol. Biol. **309:** 339–345
18 Jobling M. F., Huang X., Stewart L. R., Barnham K. J., Curtain C., Volitakis I. et al. (2001) Copper and zinc binding modulates the aggregation and neurotoxic properties of the prion peptide PrP106–126. Biochemistry **40:** 8073–8084
19 Iwai A., Masliah E., Yoshimoto M., Ge N., Flanagan L., Silva H. A. de et al. (1995) The precursor protein of non-A beta component of Alzheimer's disease amyloid is a presynaptic protein of the central nervous system. Neuron **14:** 467–475
20 George J. M., Jin H., Woods W. S. and Clayton D. F. (1995) Characterization of a novel protein regulated during the critical period for song learning in the zebra finch. Neuron **15:** 361–372
21 Uversky V .N., Li J. and Fink A. L. (2001) Evidence for a partially folded intermediate in alpha-synuclein fibril formation. J. Biol. Chem. **276:** 10733–10744
22 Eliezer D., Kutluay E., Bussel R. Jr and Browne G. (2001) Conformational properties of alpha-synuclein in its free and lipid-associated states. J. Mol. Biol. **307:** 1061–1073
23 Baba M., Nakajo S., Tu P.-H., Tomita T., Nakaya K., Lee V. M.-Y. et al. (1998) Aggregation of alpha-synuclein in Lewy bodies of sporadic Parkinson's disease and dementia with Lewy bodies. Am. J. Pathol. **152:** 879–884
24 Clayton D. F. and George J. M. (1998) The synucleins: a family of proteins involved in synaptic function, plasticity, neurodegeneration and disease. Trends Neurosci. **21:** 249–254
25 Heintz N. and Zoghbi H. (1997) Alpha-synuclein – a link between Parkinson and Alzheimer diseases? Nat. Genet. **16:** 325–327
26 Uversky V. N., Li J. and Fink A. L. (2001) Metal-triggered structural transformations, aggregation, and fibrillation of human alpha-synuclein: a possible molecular NK between Parkinson's disease and heavy metal exposure. J. Biol. Chem. **276:** 44284–44296
27 Maury C. P. J. (1995) Molecular pathogenesis of beta-amyloidosis in Alzheimer's disease and other cerebral amyloidoses. Lab. Invest. **72:** 4–16
28 Multhaup G., Beyreuther K. and Muller-Hill B. (1987) The precursor of Alzheimer's disease amyloid A4 protein resembles a cell-surface receptor. Nature **325:** 733–736
29 Bush A. I., Pettingell W. H. Jr., Multhaupt G., Paradis M. D., Vonsattel J.-P., Gusella J. F. et al. (1994) Rapid induction of Alzheimer A beta amyloid formation by zinc. Science **265:** 1464–1467
30 Bush A. I., Pettingell W. H. Jr., Paradis M. D. and Tanzi R. E. (1994) Modulation of A beta adhesiveness and secretase site cleavage by zinc. J. Biol. Chem. **269:** 12152–12158
31 Huang X., Atwood C. S., Moir R. D., Hartshorn M. A., Vonsattel J.-P., Tanzi R. E. et al. (1997) Zinc-induced Alzheimer's Abeta1-40 aggregation is mediated by conformational factors. J. Biol. Chem. **272:** 26464–26470
32 Floege J. and Ehlerding G. (1996) Beta-2-microglobulin-associated amyloidosis. Nephron **72:** 9–26
33 Prusiner S. B. (1997) Prion diseases and the BSE crisis. Science **278:** 245–251
34 Prusiner S. B. (1998) Prions. Proc. Natl. Acad. Sci. USA **95:** 13363–13383
35 Pan K.-M., Baldwin M., Nguyen J., Gasset M., Serban A., Groth D. et al. (1993) Conversion of alpha-helices into beta-sheets features in the formation of the scrapie prion proteins. Proc. Natl. Acad. Sci. USA **90:** 10962–10966
36 Brown D. R., Schmidt B. and Kretzschmar H. A. (1996) Role of microglia and host prion protein in neurotoxicity of a prion protein fragment. Nature **380:** 345–347
37 Jobling M. F., Stewart L. R., White A. R., McLean C., Friedhuber A., Maher F. et al. (1999) The hydrophobic core sequence modulates the neurotoxic and secondary structure properties of the prion peptide 106–126. J. Neurochem. **73:** 1557–1565
38 Brandner S., Isenmann S., Raeber A., Fisher M., Sailer A., Kobayashi Y. et al. (1996) Normal host prion protein necessary for scrapie-induced neurotoxicity. Nature **379:** 339– 343

39 Giese A., Brown D. R., Groschup M. H., Feldmann C., Haist I. and Kretzschmar H. A. (1998) Role of microglia in neuronal cell death in prion disease. Brain Pathol. **8:** 449–457

40 Chiti F., Webster P., Taddei N., Stefani M., Ramponi G. and Dobson C. M. (1999) Designing conditions for in vitro formation of amyloid protofilaments and fibrils. Proc. Natl. Acad. Sci. USA **96:** 3590–3594

41 Chiti F., Taddei N., Bucciantini M., White P., Ramponi G. and Dobson C. M. (2000) Mutational analysis of the propensity for amyloid formation by a globular protein. EMBO J. **19:** 1441–1449

42 Chiti F., Taddei N., Baroni F., Capanni C., Stefani M., Ramponi G. et al. (2002) Kinetic partitioning of protein folding and aggregation. Nat. Struct. Biol. **9:** 137–143

43 Pastore A., Saudek V., Ramponi G. and Williams R. J. P. (1992) Three-dimensional structure of acylphosphatase: refinement and structure analysis. J. Mol. Biol. **224:** 427–440

44 van Nuland N. A. J., Chiti F., Taddei N., Raugei G., Ramponi G. and Dobson C. M. (1998) Slow folding of muscle acylphosphatase in the absence of intermediates. J. Mol. Biol. **283:** 883–891

45 Taddei N., Stefani M., Magherini F., Chiti F., Modesti A., Raugei G. et al. (1996) Looking for residues involved in the muscle acylphosphatase catalytic mechanism and structural stabilization: role of Asn41, Thr42, and Thr46. Biochemistry **35:** 7077–7083

46 Santoro M. M. and Bolen D. W. (1988) Unfolding free energy changes determined by the linear extrapolation method. 1. Unfolding of phenylmethanesulfonyl alpha-chymotrypsin using different denaturants. Biochemistry **27:** 8063–8068

47 Brown D. R., Qin K., Herms J. W., Madlung A., Manson J., Strome R. et al. (1997) The cellular prion protein binds copper in vivo. Nature **390:** 684–687

48 Atwood C. S., Moir R. D., Huang X., Scarpa R. C., Bacarra N. M. E., Romano D. M. et al. (1998) Dramatic aggregation of Alzheimer abeta by Cu(II) is induced by conditions representing physiological acidosis. J. Biol. Chem. **273:** 12817–12826

49 Miura T., Suzuki K., Kohata N. and Takeuchi H. (2000) Metal binding modes of Alzheimer's amyloid beta-peptide in insoluble aggregates and soluble complexes. Biochemistry **39:** 7024–7031

50 Chiti F., Stefani M., Taddei N., Ramponi G. and Dobson C. M. (2003) Rationalization of the effects of mutations on peptide and protein aggregation rates. Nature **424:** 805–808

51 Creighton T. E. (1993) Proteins, Structure and Molecular Properties, p. 6, Freeman, New York

52 Harper J. D., Lieber C. M. and Lansbury P. T. (1997) Atomic force microscopy imaging of seeded fibril formation and fibril branching by the Alzheimer's disease amyloid.beta protein. Chem. Biol. **4:** 951–959

53 Halliwell B. and Gutteridge J. M. C. (1984) Oxygen toxicity, oxygen radicals, transition metals and disease. Biochem. J. **219:** 1–14

54 Steinberg D. (1995) Role of oxidized LDL and antioxidants in atherosclerosis. Adv. Exp. Med. Biol. **369:** 39–48

55 Markesbery W. R. and Carney J. M. (1999) Oxidative alterations in Alzheimer's disease. Brain Pathol. **9:** 133–146

56 O'Connel M. J. and Peters T. J. (1987) Ferritin and haemosiderin in free radical generation, lipid peroxidation and protein damage. Chem. Phys. Lipids **45:** 241–249

57 Kang J. H. and Kim S. M. (1997) Fragmentation of human Cu,Zn-superoxide dismutase by peroxidative reaction. Mol. Cells **7:** 553–558

58 Kim K. S., Choi S. Y., Kwon H., Won M. H., Kang T-C and Kang J. H. (2002) The ceruloplasmin and hydrogen peroxide system induces alpha-synuclein aggregation in vitro. Biochimie **84:** 625–631

59 Chiti F., Calamai M., Taddei N., Stefani M., Ramponi G. and Dobson C. M. (2002) Studies of the aggregation of mutant proteins in vitro provide insights into the genetics of amyloid diseases. Proc. Natl. Acad. Sci. USA **99 (suppl. 4):** 16419–16426

60 Curtain C. C., Ali F., Volitakis I. Cherny R. A., Norton R. S., Beyreuther et al. (2001) Alzheimer's disease amyloid-beta binds copper and zinc to generate an allosterically ordered membrane-penetrating structure containing superoxide dismutase-like subunits. J. Biol. Chem. **276:** 20466–20473

61 Martins R. N., Harper C. G., Stokes G. B. and Masters C. L. (1986) Increased cerebral glucose-6-phosphate dehydrogenase activity in Alzheimer's disease may reflect oxidative stress. J. Neurochem. **46:** 1042–1045

62 Multhaup G., Masters C. L. and Beyreuther K. (2000) Oxidative stress in Alzheimer's desease. Alzheimer's Rep. **1:** 147–154

63 Huang X., Atwood C. S., Hartshorn M. A., Multhaupt G., Goldstein L. E., Scarpa R. C. et al. (1999) The A beta peptide of Alzheimer's disease directly produces hydrogen peroxide through metal ion reduction. Biochemistry **38:** 7609–7616

64 Glusker J. P. (1991) Structural aspects of metal liganding to functional groups in proteins. Adv. Prot. Chem. **42:** 1–77

65 Whittal R. M., Ball H. L., Cohen F. E., Burlingame A. L., Prusiner S. B. and Baldwin M. A. (2000) Copper binding to octarepeat peptides of the prion protein monitored by mass spectrometry. Protein Sci. **9:** 332–343

66 Morita A., Kimura M. and Itokawa Y. (1994) The effect of aging on the mineral status of female mice. Biol. Trace Elem. Res. **42:** 165–177

67 Zecca L., Gallorini M., Schunemann V., Trautwein A. X., Gerlach M., Riederer P. et al. (2001) Iron, neuromelanin and ferritin content in the substantia nigra of normal subjects at different ages: consequences for iron storage and neurodegenerative processes. J. Neurochem. **76:** 1766–1773

68 Lovell M. A., Robertson J. D., Teedsdale W. J., Campbell J. L. and Markesbery W. R. (1998) Copper, iron and zinc in Alzheimer's disease senile plaques. J. Neurol. Sci. **158:** 47–52

69 Hirsch E. C., Brandel J. P., Galle P., Javoy-Agid F. and Agid Y. (1991) Iron and aluminum increase in the substantia nigra of patients with Parkinson's disease: an X-ray microanalysis. J. Neurochem. **56:** 446–451

70 Dexter D. T., Carayon A., Javoy-Agid F., Agid Y.,Wells F. R., Daniel S. E. et al. (1991) Alterations in the levels of iron, ferritin and other trace metals in Parkinson's disease and other neurodegenerative diseases affecting the basal ganglia. Brain **114:** 1953–1975

71 Tanner C. M. (1989) The role of environmental toxins in the etiology of Parkinson's disease. Trends Neurosci. **12:** 49–54

72 Rybicki B. A., Johnson C. C., Uman J. and Gorell J. M. (1993) Parkinson's disease mortality and the industrial use of heavy metals in Michigan. Movement Disorders **8:** 87–92

73 Gorell J. M., Johnson C. C., Rybicki B. A., Petrson E. L., Kortsha G. X., Brown G. G. et al. (1999) Occupational exposure to manganese, copper, lead, iron, mercury and zinc and the risk of Parkinson's disease. Neurotoxicology **20:** 239–247

74 Zayed J., Ducic S., Campanella G., Panisset J. C., Andre P., Masson H. et al. (1990) Environmental factors in the etiology of Parkinson's disease. Can. J. Neurol. Sci. **17:** 286–291